Growth of three-dimensional structures by atomic deposition on surfaces containing defects : simulations and theory

Pablo Jensen (a), Hernan Larralde (b), Muriel Meunier (a) and Alberto Pimpinelli (c)
(a) Departement de Physique des Materiaux, Universite Claude Bernard Lyon-1, 69622 Villeurbanne Cedex, FRANCE;
(b) Instituto de Fisica, Lab. de Cuernavaca, Apdo. Postal 48-3, C.P. 62251, Cuernavaca, Mor., MEXICO;
(c) LASMEA, Universite Blaise Pascal, Les Cezeaux, F-63177 Aubiere Cedex, FRANCE

We perform a comprehensive study of the formation of three dimensional (pyramidal) structures in a large range of conditions, including the possible evaporation of adatoms from the surface and the presence of surface defects. We compare our computer simulations to theoretical calculations of the growth and find good agreement between them. This work clarifies precedent studies of three dimensional growth and predicts the island size distributions obtained in the different regimes. Finally, we show how our analysis can be used to interpret experimental data.

How can one grow useful thin films or nanostructures from atomic beams? The usual and most effective way is certainly by a carefully controlled and inspired trial and error method. Theoreticians dream that another possibility may exist: by knowing the detailed atomic mechanisms that govern thin film growth, one could in principle tailor the morphologies to the desired application. Fortunately, there are many other justifications to the study of these atomic mechanisms: for example the understanding in terms of atomic mechanisms of growth experiments carried under controlled conditions, where great care is taken to avoid complications (contamination, surface defects, etc. see for example [1–6]). To be able to interpret more complex situations demands the study of models including many atomic processes [7]. The first models only included deposition, diffusion of the adatoms and their irreversible aggregation to form flat islands [8–16]. Ratsch et al. [17] improved these models by including reversible aggregation in order to reproduce the formation of compact islands. In this paper we get closer to new experimental situations by including two new ingredients: the growth of three-dimensional islands and the presence of surface defects which act as traps for the monomers, in presence of adatom evaporation.

Evaporation, i.e. the possibility of desorption of adatoms from the surface, is a feature that should be observed for any system at high enough temperatures. In this sense, it is a phenomenon that is as general as the rest of the ingredients of recent models of film growth, and, as we have shown in the case of two dimensional (2D) growth [18], is capable of completely changing the quantitative behaviour of the system. Moreover, evaporation is present in a number of experimental situations [4,19,20], where 3D islands are built. We should add that thin film growth models which include evaporation have already been studied using a mathematical analysis of rate equations [10,14–16,20–23]. Computer simulations of such models have, to our knowledge, never been carried out. The point is that computer simulations represent an "exact" way of reproducing the growth, in the sense that they avoid the mean-field approximations of rate-equations approaches [13,24,25]. We have shown previously [18] that the mean-field equations could lead to wrong predictions in the case of 2D growth: is this also the case in 3D growth?

Three-dimensional (3D) structures are often observed in the growth of heteroepitaxial and non-epitaxial films. A simple explanation of the formation of such structures, based in the bonding energies between adsorbed atoms and adsorbed atoms and the substrate can be found in [26]. We note that such thermodynamic arguments are not always trustworthy, since kinetics play an essential role in determining the growth morphologies [27–29]. We will not consider this point here and will just simulate 3D growth in a schematic way, forcing the adatoms to build pyramidal islands as they aggregate on the surface. A more realistic model should reproduce the geometric structure of the islands as a result of the different relevant energies (edge diffusion around the island, barrier for down and up-hill diffusion, ...). This is beyond the scope of the present paper where we only want to investigate the consequences of the formation of 3D structures on the growth characteristics (mainly saturation island density and island size distribution as a function of the growth parameters). The possible influence of surface defects has been stressed repeatedly [26,30,31]. We want to clarify the manifestations of defects on the growth and to check simple mathematical analysis of the growth by computer simulations.

We study here the first stages of the growth, roughly until the number of islands on the substrate saturates. The reason is that it is in this stage that such a simplified model can be of some help to experimentalists who want to understand the microscopic processes present in their experiments. These fundamental microscopic processes are most easily detected in the first stages of the growth, since in the subsequent stages additional processes can be involved (additional diffusion paths, interlayer transport, geometrical details of the lattice ...).

The paper is organized as follows. Section I briefly presents the model and discusses some of its approximations. Then, in section II, we study the growth of 3D islands, first by a simple scaling analysis in the absence of defects, then by a more rigorous mathematical mean-field treatment, where we also include the influence of surface defects which act as perfect traps on the surface. In section III, computer simulations are used to test these analytical predictions and to calculate the island size distributions in the different cases. After a discussion (section IV) where we compare our analysis to precedent studies, we show in section V how experimental results can be analyzed using these results.

I. PRESENTATION OF THE MODEL

In this work we will describe the properties of a still oversimplified submonolayer thin film growth model which includes five important physical ingredients for these systems:

(1) Deposition. We will assume that atoms are deposited at randomly-chosen positions of the surface at a flux F per unit surface per unit time. Atoms that happen to fall on the islands that are formed on the surface are accomodated at their proper pyramidal position (see below).

(2) Diffusion. Isolated adatoms can move in a random direction by one diameter, or one lattice spacing, which we will take as our unit length. We denote by τ the characteristic time between diffusion steps and $D = 1/(4\tau)$ the diffusion coefficient (the atomic size is taken as the length unit).

(3) Evaporation. Isolated adatoms can evaporate off the surface at a constant rate. We denote by τ_e the mean lifetime of a free adatom on the surface. It is also useful to define $X_S = \sqrt{D\tau_e}$, the mean adatom diffusion length before desorption

(4) Aggregation. If two adatoms come to occupy neighboring sites, they stick irreversibly and form an island. As more adatoms are captured, the island develops as a pyramid (see below). Islands are assumed to be immobile and do not evaporate.

(5) Defect trapping In some parts of the paper, we introduce a concentration c of "defects" on the surface. These defects, which are randomly distributed on the surface, act as perfect traps for the monomers. Therefore, a monomer which happens to occupy a defect remains there forever and serves as a nucleation center for island growth.

In the following, we call particles or adatoms the isolated atoms (or monomers) that are deposited on the surface, and islands a set of connected particles (thus excluding the monomers).

Some remarks on the assumptions of this simple model regarding its connection to the experiments are now addressed.

(a) Island morphology| We force the islands to assume a pyramidal shape by immediately moving an adatom that touches an island to the desired position (Fig. 1). The pyramidal shape is adopted because we wish to understand experiments carried out by one of us (MM) on the system Pd/NaCl [4] where the islands take approximately such a shape. We note that this assumption does not affect crucially the growth : it should not affect the growth exponents which are only determined by the fact that islands are three-dimensional (i.e. their mass increases as their radius to the third power, see below).

(b) Island diffusion| We neglect in this model the possibility for dimers, trimers or larger islands to diffuse on the substrate. Island diffusion has been observed in experiments [32] and molecular-dynamics simulations [33]. The effects of 2D island diffusion on the growth of thin films without evaporation have been addressed in Refs. [12,24,25,10,34,35].

II. MATHEMATICAL ANALYSIS OF THE GROWTH OF 3D ISLANDS

A. Qualitative description

Before going into the details of the calculations and their confirmation by computer simulations, we present a simple picture of the growth mechanisms of the submonolayer structures under consideration. We are interested mainly on two points : the time evolution of the island concentration on the substrate and the island concentration at saturation as a function of the growth parameters : flux, diffusion and evaporation times and defect concentration.

The qualitative evolution of the system is essentially as follows. The system initiates as a clean empty surface. Monomers are then deposited at a constant rate on the surface and are allowed to diffuse and/or desorb (evaporate). When two monomers meet, they aggregate irreversibly to form a static island (an island is also created when a monomer is trapped by a defect) : this is island nucleation. As more of these encounters occur, the island density increases with time. Competing with this nucleation process, monomers are also captured by islands which then become larger. At some point, islands are so large that they quickly capture the free monomers, which reduces the chances of two monomers meeting to nucleate a new island. Therefore, the number of islands grows less rapidly. Moreover, when islands become large, they start touching (coalescing). These two effects lead to a saturation in the number of islands. Interestingly, the saturation is attained when the surface coverage reaches a value close to .15, independently of the parameter values. This is equivalent to saying that saturation is reached when the mean island radius R is a fixed fraction of the island-island distance (the coverage is given by $\pi N R^2 \sim (R/l_{ii})^2$ where l_{ii} is the mean island-island distance). A more detailed discussion of the evolution of the system s can be done by distinguishing several cases according to the relative importance of the different phenomena : diffusion, evaporation, defect concentration. It is useful to define a typical length scale for each of these processes: $l_{cc} = (F\theta)^{1/7}$ is a typical distance between islands when evaporation and defect concentration are not important (see below), $X_S = \sqrt{D\tau_e}$ is, as defined above, the adatom diffusion length before desorption and $\ell_{def} \sim 1/c^{1/2}$ is the typical distance between defects. Now, depending on the relative values of these three length scales, growth will be dominated by different mechanisms which we turn on to describe in more detail. Note that l_{cc} corresponds to the typical island-island distance at the saturation time, i.e. it is not the actual island-island distance (for example at the beginning of film growth). Therefore our following qualitative discussion is only approximated, and the more precise calculations of later sections are necessary to justify it.

1. "Dirty" substrates : high defect concentration

By "dirty" substrate, we mean that the island concentration is affected by the defect concentration. We will show that this is true only if ℓ_{CC} is much larger than ℓ_{def}, i.e. the defect concentration is high enough, even in the absence of evaporation (if evaporation is present, it can only decrease the number of islands, therefore increasing the relative importance of defect concentration). The simplest case is when the defect concentration is very high, namely if ℓ_{def} is much smaller than both X_S and ℓ_{CC}. In this case, island nucleation is completely dominated by the trapping of adatoms by defects, which leads to two main effects : first, the island concentration reaches its saturation value rapidly (roughly in a time $c=F$); second, this saturation value is $N_{sat} = c$, i.e. all defects are occupied by islands but there are no islands created elsewhere.

Note that this situation corresponds to a "low" temperature case, when X_S is large enough. At higher temperatures, one could have $X_S \ll \ell_{def}$ (but still $\ell_{def} \ll \ell_{CC}$ to remain in the "dirty" substrate case). In this case, the monomer concentration is dominated by evaporation and island nucleation still occurs on defects. The saturation density is still equal to the defect concentration but the kinetics is different : the time needed to reach saturation is roughly $t_c \sim 1/(F(1 + X_S^2))$.

2. "Clean" substrates : low defect concentration

Here we study the cases for which the island concentration is not affected by the presence of defects, when the substrate is "clean" enough. This is true when ℓ_{CC} is much smaller than ℓ_{def}, irrespective of the X_S value. In principle, three cases can then arise, depending on the relative value of X_S against these two lengths. Our calculations will show (section IIB) that there are only two asymptotic regimes : complete condensation and high evaporation. In the complete condensation (CC) case, adatoms do not evaporate from the surface and island growth proceeds mainly by capture of the diffusing adatoms. On the contrary, in the high evaporation limit, the number of adatoms is limited by evaporation and the most important growth mechanism for islands is that of direct impingement of adatoms on top of them (the contribution from the adatoms diffusing on the surface is negligible).

The first case corresponds to $\ell_{CC} \ll X_S$, independently of the relative ordering of l_{def} and X_S. Then, adatoms almost never evaporate before aggregating (after this, they are safe since islands do not evaporate). The monomer density rapidly grows, leading to a rapid increase of island density by monomer-monomer encounter on the surface. This goes on until the islands occupy a significant fraction of the surface, roughly 1% . Then, islands capture rapidly the monomers, whose density decreases. As a consequence, it becomes less probable to create more islands, and we see that their number increases more slowly. When the coverage reaches a value close to 15% , coalescence will start to decrease the number of islands. The maximum number of islands N_{sat} is thus reached for coverages around 15% .

The second case corresponds to the opposite situation : $\ell_{CC} \gg X_S$, with still $\ell_{CC} \ll \ell_{def}$. This happens when ϵ is small, for example at high temperatures. In this regime, evaporation significantly alters the growth dynamics. The main point is that now the monomer density becomes roughly a constant (F/ϵ), since it is now mainly determined by the balancing of deposition and evaporation. Then, the number of islands increases linearly with time (the island creation rate is roughly proportional to the square monomer concentration). We also notice that only a small fraction (1/100) of the monomers do effectively remain on the substrate, as shown by the low sticking coefficient value at early times (the sticking coefficient is the ratio of particles on the substrate (the coverage) over the the total number of particles sent on the surface (Ft)). This can be understood by noting that an island of radius R grows by capturing only the monomers that are deposited within its "capture zone" (the circle of radius $R + X_S$ centered on island's center). The other monomers evaporate before reaching the islands. As in the case of complete condensation, when the islands occupy a significant fraction of the surface, they capture rapidly the monomers. This has two effects : the monomer density starts to decrease, and the sticking coefficient starts to increase. Shortly after, the island density saturates and starts to decrease because of island-island coalescence.

Note that one could have in principle $X_S \ll 1$, i.e. the adatoms evaporate before diffusing. This situation, although apparently uncommon, is not physically impossible and it also allows us to test our predictions over a larger range of parameters. We note that, in contrast to what is observed for two dimensional (2d) islands [18], particles deposited on top of islands significantly contribute to island growth. In presence of strong evaporation, this is actually the dominant mechanism for island growth, whereas for the 2d case this happens only in some special regimes [18].

3. Summary of our results

We present here the summary of our results in the different limits described above. These results are derived in detail in sections IIB and IIC. For each regime, we give in the order the saturation island density N_{sat}, the thickness at saturation e_{sat} (i.e. the thickness when the island density first reaches its saturation value), the thickness at coalescence e_c (i.e. the thickness when the island density starts to decrease due to island-island coalescence), and the scaling kinetics of the mean radius as a function of time before the saturation island density is reached. We recall that $l_{CC} = (F)^{1/7}$ and $X_S = \sqrt{D_e/F}$.

Clean substrate

high evaporation : $X_S \ll l_{CC} \ll l_{def}$

$N_{sat} \sim [F\tau_e(1+X_S^2)]^{2/3}$

$e_{sat} \sim e_c \sim [F\tau_e(1+X_S^2)]^{1/3}$

$R \sim Ft$

low evaporation : $l_{CC} \ll X_S \ll l_{def}$ or $l_{CC} \ll l_{def} \ll X_S$

$N_{max} \sim \left(\frac{F}{D}\right)^{2/7}$

$e_{sat} \sim e_c \sim \left(\frac{D}{F}\right)^{1/7}$

$R \sim (FDt^2)^{1/9} \sim t^{2/9}$

Dirty substrate

high evaporation : $X_S \ll l_{def} \ll l_{CC}$

$N_{max} \sim c$

$e_{sat} \sim \frac{1}{[1+X_S^2]}$

$e_c \sim \frac{1}{c^{1/2}}$

$R \sim Ft$

low evaporation : $l_{def} \ll X_S \ll l_{CC}$ or $l_{def} \ll l_{CC} \ll X_S$

$N_{max} \sim c$

$e_{sat} \sim c$

$e_c \sim \frac{1}{c^{1/2}}$

$R \sim \frac{Ft}{c}$ for $t \ll c/F$, i.e. before saturation

$R \sim (Ft/c)^{1/3}$ between saturation and coalescence ($c/F \ll t \ll 1/Fc^{1/2}$), see section IIC.

B. Scaling arguments for defect-free ("clean") surfaces

In this section we present simple scaling arguments that allow to find the dependence of the maximum island density N_{max} as a function of the deposition parameters (Flux F, Diffusion time τ and Evaporation time τ_e). These arguments were originally formulated in [10] for the special case of growth of 2D islands by atom deposition on a high-symmetry terrace, neglecting evaporation. Here, the argument is extended to the case of non-negligible evaporation. We recall that the atomic size is taken as the length unit.

The first stage of the argument requires the determination of the nucleation rate per unit surface and time, $1/\tau_{nuc}$. A nucleation event takes place when an adatom meets a critical island of size s. We call N_s the density of critical nuclei (clusters of size s) and, following Refs. [22,23], we assume that N_s satisfies Walton's relation $N_s \sim \tau^{-s}$. Thus,

$$\frac{1}{\tau_{nuc}} \sim (F + D)N_s \qquad (2.1)$$

where $D = 1/(4\ )$ is the adatom diffusion constant. The term $F N_s$ accounts for direct impingement of atoms onto critical islands and the second term for critical island growth by monomer diffusive attachment.

Another, independent equation can be written down to relate the nucleation rate and the stable ($s < s$) island density N. It states that in the area $\ell_s^2 = 1/N$ occupied by an island, only one (on average) nucleation event takes place, during the time t_c needed for the growing islands to come into contact. Thus,

$$\frac{1}{\ _{nuc}} \quad \frac{N}{t_c} : \tag{2.2}$$

The time t_c is readily computed by knowing the growth velocity of an island, which in turn requires the knowledge of the adatom density. We consider in the following three situations of interest for this paper.

1. Negligible evaporation

.

The adatom density results in this case from a balance between deposition at a rate F and capture by the stable islands at a rate $D\ N$, so that

$$F = (D\ N) \quad F\ \ell_s^2/D : \tag{2.3}$$

The rate of growth of the volume of an island of linear size R is diffusion-limited in this case, so that $d(R^3)/dt \quad D$ and $R^3 \quad F t/N$. At $t = t_c$, $R \quad \ell_s$, and thus

$$t_c \quad N\ \ell_s^3/F \quad 1/(F N^{1/2}) : \tag{2.4}$$

Using (2.1) and (2.3), one finds

$$\frac{1}{\ _{nuc}} \quad D\ [F/(D\ N)]^{s+1} \tag{2.5}$$

(here, the direct impingement term is negligible).

From (2.2) and (2.4),

$$\frac{1}{\ _{nuc}} \quad F N^{3/2} : \tag{2.6}$$

Finally, (2.5) and (2.6) yield [22,23]

$$N \quad \left(\frac{F}{D}\right)^{2s/(2s+5)} : \tag{2.7}$$

2. Strong evaporation

.

Strong evaporation means the adatoms are more likely to disappear due to desorption than to be captured by an island. In other words, the adatom diffusion length before desorption, $X_S = \sqrt{D\ _e}$, is shorter than the average island-island distance, ℓ_s. In this case, the adatom density results from a balance between deposition and desorption at a rate $\ = \ _e$, so that

$$F \ _e \quad F X_S^2/D : \tag{2.8}$$

A 3-D island grows by two mechanisms in the case of strong evaporation: (i) by capture of the adatoms falling on the surface at a distance smaller than X_S; (ii) by direct capture of all adatoms falling on it. Thus, $dR^3/dt \quad F(X_S R + X_S^2 + R^2) \quad F(R^2 + X_S R)$. Solving for R with the condition $R = 0$ at $t = 0$, one gets $R \quad X_S \ln(1 + R/X_S) = F t$. At $t = t_c$, $R \quad \ell_s > X_S$, which means that direct capture always dominates. It follows $F t_c \quad \ell_s$, or

$$t_c \quad 1/[F N^{1/2}] : \tag{2.9}$$

Using (2.1) and (2.8), one finds

$$\frac{1}{\tau_{nuc}} \quad (F + D\ )^{s} \quad F\,(1 + X_S^2)^{s} \quad F\,(1 + X_S^2)(F\ _e)^{s} \ : \tag{2.10}$$

From (2.2) and (2.9),

$$\frac{1}{\tau_{nuc}} \quad F N^{3=2} \ : \tag{2.11}$$

Finally, (2.10) and (2.11) yield

$$N \quad (F\ _e)^{2s\ =3}\ \left(1 + X_S^{2\ }\right)^{2=3} \ : \tag{2.12}$$

We discuss the preceding results in section IV.

3. Crossover between the two preceding regimes

We will show in this section that it is possible to derive interpolation formulae describing the crossovers between the no-evaporation and the strong-evaporation regimes.

To do this, we will use Burton, Cabrera and Frank's theory of step flow [36]. The adatom density will be computed on a terrace bounded by two parallel steps, at a distance ℓ. They may be the steps in the ordered array of a vicinal surface; in this case, we will let $\ell = d$. Or they may represent the edges of a big enough island; in the latter case we will let $\ell = \ell_s = 1/\sqrt{N}$.

The adatom density obeys the equation

$$\dot{n} = F + D\nabla^2 n \quad \frac{n}{\tau} \ : \tag{2.13}$$

The time τ is the average lifetime of an adatom. Since adatoms disappear either by capture by islands, or by desorption, we will alternatively let $1/\tau = DN = D/\ell_s^2$ or $1/\tau = 1/\tau_e = D/X_S^2$. In both cases, the notation $\ell^2 = 1/(DN)$ will be used.

In the quasi-stationary approximation [36], $\dot{n} \simeq 0$, and choosing the origin $x = 0$ at the terrace centre, equation (2.13) can be solved with the conditions $n(\pm\ell/2) = 0$ at boundary steps. The solution reads

$$n(x) = F\tau \quad 1 \quad \frac{\cosh(x/\ell)}{\cosh(\ell/2\ell)} \ : \tag{2.14}$$

This formula will be needed to compute the nucleation rate (2.1). The latter is an average quantity, independent of x. We let thus $x = 0$ in (2.14), since the higher nucleation probability is at the terrace centre, given the symmetry of our problem. One finds

$$n = F\tau \quad 1 \quad \frac{1}{\cosh(\ell/2\ell)} \ = 2F\tau \ \frac{\sinh^2(\ell/4\ell)}{\cosh(\ell/2\ell)} \ ; \tag{2.15}$$

where we used the identity $\cosh(x) \quad 1 = 2\sinh^2(x/2)$.

The next task is the determination of the island density. To this end, it suffices to consider the total island density N. Its time variation is simple: N increases each time a new island is nucleated, so $(\dot{N})_1 = D\ N_s$. On the other hand, N decreases when two islands touch and coalesce. Following the authorities [22,23], we write $(\dot{N})_2 = \quad (dA/dt)N^2$, where $A \quad R^2$ is the average area of an island of linear size R. This means that coalescence results from binary encounters of immobile islands, whose area increases at a rate dA/dt. Collecting $(\dot{N})_1$ and $(\dot{N})_2$ yields

$$\dot{N} = D\ N_s \quad \frac{dA}{dt} N^2 \ : \tag{2.16}$$

At stationarity, which is what we are interested in, $\dot{N} = 0$. Note that, by definition, coalescence takes place when $A \quad \ell_s^2$. One can thus write

$$D\ N_s \quad \frac{dA}{dt}_{A\ \ell_s^2} N^2 \ : \tag{2.17}$$

The final task concerns therefore the evaluation of the growth rate of an island. This can be done by noting that the mass M of an island increases either by direct capture of atoms from the beam, or by diffusion of adatoms on the surface. Since the surface diffusion current of adatoms is $-D\nabla n$, assuming circular ($d = 2$) or hemispherical ($d = 3$) islands of radius R one can write

$$\frac{dM}{dt} \sim FR^{d-1} - D\left(\frac{dn}{dr}\right)_R . \tag{2.18}$$

The result can be found in a number of papers [18,22,23,36]. It makes use of Bessel functions, which are not easy to manipulate. Approximate results, which have the merit of reproducing the correct limiting regimes (see below), and of allowing analytical expressions to be written down, will be used.

The adatom density is still given by Eq.(2.15), and the nucleation rate by Eq.(2.1). The growth rate of the (projected) area of a 3-D island has two contributions, as for 2-D islands: a diffusion-limited contribution, which is given by

$$\frac{dA}{dt}\Big|_{R=\ell_s} \sim FX_S\ell_s \tanh(\ell_s/2), \tag{2.19}$$

and a direct capture contribution,

$$\frac{dA}{dt}\Big|_{R=\ell_s} \sim F\ell_s^2 . \tag{2.20}$$

A useful interpolation formula between (2.19) and (2.20) is

$$\frac{dA}{dt}\Big|_{R=\ell_s} \sim F\ell_s^2\left(1+\frac{X_S}{\ell_s}\right)\tanh(\ell_s/2). \tag{2.21}$$

Finally, (2.2) and (2.21) yield

$$\frac{(1+X_S)^2}{\epsilon} \sim F\epsilon\left(\frac{\sinh^2(\ell_s/4)}{\cosh(\ell_s/2)}\right)^{s+1} \sim F\ell_s^2\left(1+\frac{X_S}{\ell_s}\right)\tanh(\ell_s/2)N^2, \tag{2.22}$$

or,

$$(1+X_S)^2(F\epsilon)^s \sim \left(\frac{\cosh(N^{-1/2}/2)}{\sinh^2(N^{-1/2}/4)}\right)^{s+1}\tanh(N^{-1/2}/2)(1+X_SN^{-1/2})N^{-3/2}. \tag{2.23}$$

Multiplying both sides by X_S^3 yields

$$X_S^{2s+3}(1+X_S^2)(F/D)^s \sim f(X_SN^{-1/2}), \tag{2.24}$$

where

$$f(x) = \left[\frac{\cosh\frac{1}{2x}}{\sinh^2\frac{1}{4x}}\right]^{s+1}\tanh\frac{1}{2x}\,(1+x)x^3 . \tag{2.25}$$

Letting $N_{3D\,evap} = FX_S^2/D\left(2s+3\right)^{2s/3}\left(1+X_S^2\right)^{2/3}$, formula (2.24) can be cast in the form

$$\tilde{f}_{3D\,evap}(X_S^2N) = X_S^2N_{3D\,evap}, \tag{2.26}$$

where $\tilde{f}_{3D\,evap}(x) = [f(x^{1/2})]^{2/3}$. Inverting $\tilde{f}(x)$ yields the crossover scaling function

$$X_S^2N = g_{3D\,evap}(X_S^2N_{3D\,evap}). \tag{2.27}$$

The function $g_{3D\,evap}(x)$ has the following properties:

$$g_{3D\,evap}(x) \sim \begin{cases} x^{3/(5+2s)} & \text{for } x \to \infty, \\ x & \text{for } x \to 0. \end{cases} \tag{2.28}$$

C. Rate equations

In this section we study the growth in presence of defects using rate equations [37].

We will consider that the islands are semi-spherical "droplets" as a result of "fast" large scale reacomodation of the monomers forming the island. In addition to evaporation, we will also consider the effects due to the presence of point defects on the surface. We will assume that these defects serve as perfect nucleation points, and so, as the concentration of defects increases, the system passes from homogeneous to heterogeneous nucleation.

We can write the evolution of the density ρ of monomers on the surface as:

$$\frac{d\rho}{dt} = F - \rho/\tau_e - F\sigma_o(2\rho + c_{def}) - \sigma_i N\rho. \tag{1}$$

The first term on the RHS denotes the flux of monomers onto the surface. The second term represents the effect of evaporation. The third term is due to the possibility of losing monomers by effect of direct impingement of a deposited monomers right beside a monomer still on the surface to form an island. The next terms represent the loss of monomers by aggregation with other monomers, nucleation on defects and aggregation with islands respectively. The factors σ_o and σ_i are the "cross sections" for encounters and are detailed below.

The number N of islands will be given by:

$$\frac{dN}{dt} = F(\rho + c_def)\rho + \sigma_o(\rho + c_{def})\rho \tag{2}$$

where the first term represents the formation of islands due to direct impingement of deposited monomers onto other monomers or defects, and the second term accounts for the formation of islands by the encounter of two monomers diffusing on the surface, or a monomer on a defect. It should be noted that since this description yields scaling results, some numerical factors are omitted.

The concentration of "free defects" varies as

$$\frac{dc_{def}}{dt} = -(\sigma_o\rho + F)c_{def}.$$

The total island mass density (M) changes as

$$\frac{dM}{dt} = 2[F\rho + \sigma_o\rho^2]\rho + \sigma_i N\rho + \sigma_o c_{def}\rho + F\pi R^2 N, \tag{5}$$

where the direct impingement term is proportional to the area of the islands.

The typical island radius R will be given by

$$R \sim \left(\frac{M}{N}\right)^{1/3}, \tag{6}$$

and the actual island coverage will then be

$$N\pi R^2 = (N\pi M^2)^{1/3}. \tag{7}$$

The expressions for the diffusive cross sections in the presence of evaporation were calculated in [18].

$$\sigma_i \sim \begin{cases} \frac{D\tau}{X_S} & \text{for } R >> X_S, \\ D & \text{for } R << X_S. \end{cases} \tag{12}$$

Where $X_S = \sqrt{D\tau_e}$ is the typical distance traveled by a diffusing particle on the surface before it desorbs. And:

$$\sigma_o \sim D. \tag{13}$$

These mean-field cross sections only depend on the radius of the sphere touching the surface, and not on the height of the island, therefore they are the same for 2d or 3d particles of same radius.

As the most we can expect to obtain from this description are the scaling behaviors, we focus only on the extreme limiting cases of the system described by the rate equations.

For the case of negligible evaporation and high enough initial concentration of defects, we expect the equations to reduce to

$$\frac{d}{dt} \quad F \quad D \quad (c_{def} + N):$$

$$\frac{dN}{dt} \quad D \quad (+ c_{def})$$

$$\frac{dc_{def}}{dt} = \quad D \quad c_{def}:$$

Adding the second and last equations, we have:

$$\frac{d(N + c_{def})}{dt} \quad D \quad ^2:$$

For high enough initial concentration of defects c, we can write

$$N(t) \quad c \quad c_{def}(t) + D\,(\frac{F}{D\,c})^2 t \quad c$$

$$\frac{F}{D\,c}$$

$$c_{def}(t) \quad ce^{\frac{F\,t}{c}}:$$

The island density at saturation is therefore equal to the initial defect concentration c. To find what is "high enough" for the defect concentration, we note that nucleation events start to reduce the number of islands roughly when the island size is of the order of the distance between islands, or equivalently, when the coverage reaches a constant value. Since the deposited mass grows as $F\,t$ (evaporation is negligible), the surface coverage will be given by

$$N^{1=3}(F\,t)^{2=3} \quad (cF^2t^2)^{1=3}$$

Thus, the coalescence time is $t_c \quad 1=(F\,c^{1=2})$ and the cross over to the "clean system" occurs when

$$(\frac{F}{D\,c^{5=2}}) \quad c \quad \text{i.e.:} \quad c \quad (F=D)^{2=7}:$$

It should be stressed that in this defect dominated, or "dirty", regime the island number density saturates far before coalescence, indeed the saturation time t_s can be estimated by the characteristic time for defect ocupation: $t_s \quad c=F$. After t_s, the island density remains essentially constant and the islands grow (the typical island radius can be easily shown to grow as $R \quad (F\,t=c)^{1=3}$) until coalescence.

At high evaporation rates the aggregation of mass on the surface is dominated by "direct impingement" of particles on the islands, and the concentration of monomers on the surface is determined by the balance between deposition and evaporation. Under these conditions, at high initial defect concentration we will have:

$$F \quad _e$$

$$\frac{dN}{dt} \quad F \quad _eD\,c_{def} + F^2 \quad _e + D\,F^2 \quad ^2_e$$

$$\frac{dc_{def}(t)}{dt} \qquad F\,(D_e + 1)c_{def}$$

These equations can be solved immediately, from which we get:

$$c_{def} \quad ce^{\,[X_s^2+1]Ft]}$$

and

$$N \quad c[1 \quad e^{\,[X_s^2+1]Ft]}] + F^2 e[X_s^2 + 1]t;$$

where we have substituted $X_s = \sqrt{D_e}$.

From these expressions it is evident that the time at which N saturates is $t_s \quad 1=(F[1+X_s^2])$, after which time, the island density reaches the value N c (this, of course, assuming that the homogeneous contributions are negligible throughout the evolution of the system). It is then straightforward to find that the mass deposited on the system grows as M cF^3t^3 and the typical island radius R Ft. The coverage increases as cF^2t^2, from which we can estimate the coalescence time $t_c \quad 1=Fc^{1=2}$. While it can be imagined that these times could occur in the wrong order, we have checked that for this to be the case, an initial concentration of defects larger than one would be required.

By comparing the maximum value of the subdominant homogeneous term with c, we can determine that this high evaporation dirty regime is attained when $c >> (F e[1+X_s^2])^{2=3}$.

Finally, for completeness, we sketch the derivation of the results for the "clean" substrate with negligible evaporation. Under these circumstances, the monomer density on the surface is determined by the balance between deposition and diffusive capture by the islands on the surface. Thus, the monomer and island densities are given by

$$\frac{F}{DN} \qquad \text{and} \qquad \frac{dN}{dt} \quad D \quad \frac{F^2}{DN^2}:$$

From these equations we find that the island density is $N \quad (F^2t=D)^{1=3}$. Also, as we are considering the case of negligible evaporation, the mass deposited on the surface will be M Ft. From these quantities we can infer the behavior of the typical island radius to be given by $R \quad (M=N)^{1=3} \quad (DFt^2)^{1=9}$, and the saturation and coalescence times to be $t_c \quad t_s \quad (D=F^8)^{1=7}$, at which times the maximum value of N is $N_{max} \quad (F=D)^{2=7}$, as obtained in the previous section.

III. COMPUTER SIMULATIONS

In the following paragraphs, we test the assumptions and predictions of the analysis given in the preceding sections. We also show results that are not attainable from this mean-field calculations, namely the island size distributions.

Our computer simulations generate sub-monolayer structures using the four processes included in our model (see the introduction). Here we take = 1 as the time scale of our problem. The monomer diffusion coefficient is then given by D = 1=4. We use triangular lattices (six directions for diffusion) of sizes up to 2000 2000 with periodic boundary conditions to limit finite size effects.

The program actually consists of a repeated loop. At each loop, we calculate two quantities $p_{drop} = F=(F + (\frac{1}{e} + \frac{1}{})))$ and $p_{dif} = (=)=(F + (\frac{1}{e} + \frac{1}{}))$ that give the respective probabilities of the three different processes which could happen : depositing a particle (deposition), moving a particle (diffusion) or removing a particle from the surface (evaporation). More precisely, at each loop we throw a random number p ($0 < p < 1$) and compare it to p_{drop} and p_{dif}. If $p < p_{drop}$, we deposit a particle; if $p > p_{drop} + p_{dif}$, we remove a monomer, otherwise we just move a randomly chosen monomer. After each of these possibilities, we check whether an aggregation has taken place and go to the next loop (for more details, see [12]).

1. Checking the crossover scaling

Before looking in detail into the different regimes predicted in section IIC, we summarize our simulation results in Fig. 2. We show there all our data for N_{max} as a function of the parameters. Our scaling analysis predicts that the data should fall into a single curve, given by Equation 2.28. We see that the data remarkably confirms our analysis, over more than 30 orders of magnitude. This gives us confidence on our entire approach and its predicted exponents, which we now turn on to check in more detail.

We now check that the results summarized in section IIA 3 are correct.

2. Scaling of the maximum island density as a function of incident flux

Figure 3 shows the evolution of the maximum island density as a function of the flux for different evaporation times. Each of these curves is different from the others, since they correspond to different evaporation times. However, according to our preceding analysis, they should all present a transition from the low evaporation regime to the high evaporation regime. This can be detected by a change of slope, from $N_{max} \propto F^{2/3}$ in the high evaporation regime (solid line) to $N_{max} \propto F^{2/7}$ in the low one (dashed line). Of course, this regime change does not occur for all the curves at the same value of the Flux, since the parameter that determines that change is not the Flux but rather $X_S^2 = \tau_e/\tau$. Figure 3 shows that the results of section IIA 3 accurately describes the behaviour of our model, at least concerning the Flux evolution of the maximum island density. We now turn to the other variable, the evaporation time.

3. Maximum island density as a function of evaporation time

We show in Figure 4 the dependence of the maximum island density on τ_e ($\theta = 1$). We notice that for high enough evaporation times, the island density tends to become roughly constant, as predicted by our calculations. For lower values of τ_e, N_{max} changes rapidly. We predict (section IIA 3) two regimes : for $1 \ll \tau_e \ll F^{-1/3}$, we expect $N_{max} \propto \tau_e^{4/3}$, while for $\tau_e \ll 1$, we expect $N_{max} \propto \tau_e^{2/3}$. This last regime is clearly seen for the curves obtained for fluxes $F = 10^{-6}$ and $F = 10^{-4}$ (squares and diamonds respectively, the slope 2/3 is given by the solid line). The first regime is difficult to see for two reasons. First, we need $X_S \gg 1$ and strong evaporation, i.e. $\ell \ll X_S$. This means a very low island density, meaning very long computing times and large lattices. Second, the crossovers with the two other regimes (exponents 2/3 and 0) tend to mask the exponent 4/3. Taking a lower value for the flux ($F = 10^{-8}$, filled circles), we can see that the slope in this intermediate regime is larger than 2/3.

4. Mean island radius versus time for clean substrates

Our treatment predicts two limiting regimes for the power-law ($r \propto t^{\alpha}$) evolution of the mean island radius as a function of time : $\alpha = 1$ in cases of strong evaporation and $\alpha = 2/9$ for complete condensation (we only treat here the case of "clean" substrates"). Fig. 5a shows that we observe indeed an exponent very close to $2/9 = 0.22$ when evaporation is negligible ($X_S = 10^9; \ell_{CC} = 37$, $X_S \gg \ell_{CC}$), while the exponent is close to 1 in the opposite case ($X_S = 1; \ell_{CC} = 14$, $X_S \ll \ell_{CC}$), see Fig. 5b. Of course, intermediate cases can arise in experiments and the exponent is between these two extreme values, with values around 0.5-0.6 as shown in Fig. 5c ($X_S = 10; \ell_{CC} = 27$). Note that we have defined here the radius as $(M/N)^{1/3}$ where M is the total mass present on the substrate and N the island density, but we have checked that similar exponents are measured if one defines the mean radius as $\theta/N^{1/2}$ where θ is the surface coverage.

5. Dynamical evolution of island density

Here we investigate how the different microscopic mechanisms can affect the growth kinetics. This can be an important help for experimentalists seeking information on which processes are actually present in their experiments [38]. Fig. 6 confirms our analytical analysis and shows that evaporation or the presence of surface defects can significantly alter the time evolution of island density. If defects are present, monomers will be trapped by them at the very beginning of the growth and the number of islands equates rapidly the number of defects, whatever the diffusivity of the atoms. If evaporation is present, the opposite effect is observed : since many atoms do not contribute to the growth (they evaporate before reaching an island), the saturation is reached for very high thicknesses (typically $\theta_{sat} \gg 1$ ML).

6. Island size distributions

Island size distributions have proven very useful as a tool for experimentalists to distinguish between different growth mechanisms [39,40]. By size of an island, we mean the surface it occupies on the substrate. For the "three dimensional" particles studied here, their projected surface is the easiest quantity to measure by microscopy. Note that the projected surface for a given mass depends on the precise shape of the islands, which is assumed here to

be pyramidal (close to a half-sphere). Size distributions are normalized by the mean island size in the following way : one defines $p(s/s_m) = n_s/N_t$ as the probability that a randomly chosen island has a surface s when the average surface per island is $s_m = /N_t$, where n_s stands for the number of islands of surface s, N_t is the total number of islands and for the coverage of the surface. It has been shown [11] that by normalizing the probabilities and plotting $s_m \quad p(s/s_m)$ against s/s_m, one obtains a "universal" size distribution independent of the coverage, the ux or the substrate temperature for a large range of their values. These size distributions can be obtained from the simulations [18,24,25,41].

Fig 7 shows the evolution of the rescaled island size distributions for three dimensional islands (pyramids) in presence of evaporation. We recall that size means here the projected surface of the island, a quantity which can be measured easily by electronic microscopy. We note the same trends as for 2d islands [18]. It is clear that the distributions are significantly affected by the evaporation, smaller islands becoming more numerous when evaporation increases. This trend can be qualitatively understood by noting that new islands are created continuously when evaporation is present, while nucleation rapidly becomes negligible in the complete condensation regime. The reason is that islands are created (spatially) homogeneously in the last case, because the positions of the islands are correlated (through monomer diusion), leaving virtually no room for further nucleation once a small portion of the surface is covered (0:05). In the limit of strong evaporation, islands are nucleated randomly on the surface, the uctuations leaving large regions of the surface uncovered. These large regions can host new islands even for relatively large coverages, which explains that there is a large proportion of small ($s < s_m$) islands in this regime.

Fig 8 shows the evolution of the rescaled island size distributions for pyramidal islands nucleating on defects. Two main dierences can be noted. First, the histograms are significantly narrower than in the preceding case, as had already been noted in experimental studies [31]. This can be understood by noting that all islands are nucleated at almost the same time (at the very beginning of growth). The second point is that the size distributions are sensitive to the actual coverage of the substrate, in contrast with previous cases. In other words, there is no perfect rescaling of the data obtained at dierent coverages, even if rescaling for dierent uxes or diusion times has been checked.

IV. DISCUSSION

Other authors have analyzed similar mean-field rate equations to find the growth dynamics and maximum island density in the presence of evaporation [20–23]. They have also obtained dierent regimes identified roughly in the same way as in the present work. We think that there is some ambiguity in their definition of the dierent regimes. A regime – meaning a single relation between N_{max} and the deposition parameters – should be defined only by the values of F, $_e$ and , as in Section IIA 3. This is what is required from the experimental side : given some values of the parameters, what will happen on the surface? Instead, previous works have introduced other parameters, such as the coalescence coverage, the capture cross sections, or even the island density itself, in the characterization of the regimes.

Besides this general remark, we note that there is some disagreement about the dierent regimes between the various authors. Stoyanov and Kashchiev [23] find two regimes which correspond to our complete condensation and strong evaporation (with $X_S \quad 1$) cases. We have added here the case $X_S \quad 1$. Venables et al. [22] find three dierent regimes. The two extreme regimes coincide with Stoyanov's and ours, but their intermediate regime (which predicts $N_{max} \quad (F_e)^{2=5}$ is not observed in our simulations : this is particularly clear in Fig. 4 which shows no $_e^{2=5}$ dependence : instead, the intermediate regime shows an exponent greater than 2/3, as predicted by Eq. 2.12). Actually, Venables's intermediate regime seems physically strange because there is no dependence on the diusion coefficient of the adatoms.

The time evolution of the mean radius has also been studied previously (for a recent review, see [42] and references therein). Here, we have shown that the exponent of the radius versus time power-law is 1 when evaporation is important (islands grow only by direct impingement), 1/3 when condensation is almost complete and the number of islands is constant (for example when their concentration reaches the defect concentration for "dirty" substrates) or 2/9 for clean substrates and complete condensation (here the number of islands is never really constant since nucleation does not stop until coalescence).

In previous studies [42], it has been predicted that the radius shows a power-law dependence with an exponent 1/3 for complete condensation growth and 1 in the case of strong evaporation. Intermediate values were found thanks to the numerical resolution of mean-field equations of island growth [42].

The experimental values are rather in the range 0.21 – 0.30 for the Pd/MgO (100) system [42] and around 0.3 in other systems. While the intermediate exponents (between 1/3 and 1) can be explained as pertaining to the intermediate regime (see section III 4), the values lower than 1/3 are more difficult to explain. In our analysis, the exponents close

to 2/9= 0.22 can simply be explained (in the complete condensation regime and for clean substrates) by the fact that the island density is not constant (as assumed in previous studies).

V. INTERPRETATION OF EXPERIMENTAL DATA

In principle, Figure 3 allows to determine the value of the microscopic parameters (diffusion, evaporation) if the saturation island density is known. The problem is : does this island density correspond to the defect concentration of the surface or to homogeneous nucleation? Is evaporation present in our experiments and what is the magnitude of $_e$?

The first question can be answered by looking at the density evolution with the flux. As already explained, if this leaves unaffected the island density, nucleation is occuring on defects. A similar test can be performed by changing the substrate temperature, but there is the nagging possibility that this changes the defect concentration on the surface. It is also possible to study the kinetics of island nucleation, i.e. look at the island concentration as a function of thickness or coverage. The presence of defects can be detected by the fact that the maximum island density is reached at very low coverages (typically less than 1% , see Fig. 6). One should be careful however to check that all the islands, even those containing a few atoms, are visible in the microscope images.

The second question is more delicate. First, one should check whether atomic reevaporation is important. In principle, this can be done by measuring the sticking coefficient, i.e. the amount of matter present on the surface as a function of the matter brought by the beam . If possible, this measure leaves no ambiguity. Otherwise, the kinetics of island creation is helpful. If the saturation is reached at low thicknesses (e_{sat} :5 ML), this means that evaporation is not important. Another way of detecting atom evaporation is by studying the evolution of the saturation island density with the flux : the exponent goes from 0.29 to 0.66 (Fig. 3). Suppose now that one finds that evaporation is indeed important : before being able to use Fig. 3, one has to know the precise value of $_e$, and this is not easily achieved. For example, one could try to measure the sticking coefficient or the quantity of matter needed to reach saturation to obtain an estimation of the evaporation. Intuitively, the more evaporation is important, the more matter we need to reach the saturation density. Unfortunately, this strategy, although useful for growth of 2d islands [18] is not so straightforward here. The reason is that in the limit of strong evaporation (section IIB 2), one has e_{sat} N_{sat} $^{1=2}$, thus bringing no independent information on the parameters. The same is true for the sticking coefficient, which is a constant, i.e. independent of the value of $_e$ or the normalized flux. This counterintuitive result can be understood by noting that in this limit, islands only grow by direct impingement of atoms within them . Fortunately, in many experimental situations the limit of high evaporation is not reached and we "benefit" from (mathematical) crossover regimes where these quantities do depend on the precise values of $_e$. Fig. 9 gives the evolutions of S_{sat} and e_{sat} for different values of $_e$ and F in this crossover region. Then, a measurement of S_{sat} or e_{sat} can shed light on experimental the value of $_e$. For more details on interpretation of experimental data, we refer the reader to a review paper to appear [38].

VI. SUMMARY, PERSPECTIVES

We have presented a comprehensive theoretical analysis of the growth of three dimensional structures on surfaces by atom evaporation. The study has been carried out by combining a simple scaling analysis, a more rigorous rate equations approach and computer simulations, with the main scope of helping experimentalists to analyze their data. The scaling analysis can give very simply the growth exponents in the "clean" substrate case, in the limiting regimes of high and low evaporation as well as in the crossover between these. The rate equations confirm this analysis and predict the growth on "dirty" substrates, i.e. surfaces containing perfect traps for adatoms. The two approaches were compared to Monte-Carlo computer simulations and very good agreement was found. In addition to the analytical predictions, computer simulations allowed to predict for the first time important growth characteristics such as the island size distributions and intermediate regimes which are difficult to study analytically. This is particularly interesting for the interpretation of experimental data from the the sticking coefficient and the saturation island density (see section V).

We wish to thank C. Henry for helpful discussions.

e-mail addresses : jensen@dpm.univ-lyon1.fr, hernan@cce.isicam.unam.mx, Alberto.Pimpinelli@lasmea.univ-bpclermont.fr

[1] Y.W. Mo, J. Kleiner, M.B. Webb and M.G. Lagally, Phys. Rev. Lett. 66, 1998 (1991).
[2] H. Roder, E. Hahn, H. Brune, J.-P. Bucher, and K. Kern, Nature 366, 141 (1993); H. Brune, C. Romainczyk, H. Roder, and K. Kern, Nature 369, 469 (1994); H. Brune, H. Roder, C. Boragno, and K. Kern, Phys. Rev. Lett. 73, 1955 (1994)
[3] R.Q. Hwang, J. Schroder, C. Gunther and R.J. Behn, Phys. Rev. Lett. 67, 3279 (1991); T. Michely, M. Hohage, M. Bott, and G. Comsa, Phys. Rev. Lett. 70, 3943 (1993)
[4] M. Meunier, PhD thesis (Universite Aix-Marseille, 1995); M. Meunier and C.R. Henry, Surf. Sci. 307, 514 (1994)
[5] For recent experimental results, see for example Evolution of Epitaxial Structure and Morphology, ed. A. Zangwill, D. Jesson, D. Chambliss and R. Clarke, or Disordered Materials and Interfaces - Fractals, Structure and Dynamics, ed. H.E. Stanley, H.Z. Cummins, D.J. Durian and D.L. Johnson, both Proceedings of the Materials Research Society, Fall Meeting, Boston, December 1995, volumes 399 and 407 respectively.
[6] Proceedings of the 14th European Conference on Surface Science (September 1994), Surface Science 331-333 (1995).
[7] To help experimentalists, a software simulating the submonolayer regime of thin-film growth in the various growth hypothesis (2d or 3d islands, reversible aggregation, mobile islands ...) is presently being developed and will soon be available by simple request to one of us (PJ).
[8] M. Lagally, Physics Today 46(11), 24 (1993) and references therein.
[9] L.-H. Tang, J. Phys. I France 3, 935 (1993)
[10] J. Villain, A. Pimpinelli, L.-H. Tang, and D.E. Wolf, J. Phys. I France 2, 2107 (1992); J. Villain, A. Pimpinelli and D.E. Wolf, Comments Cond. Mat. Phys. 16,1 (1992)
[11] J.W. Evans and M.C. Bartelt, J. Vac. Sci. Technol. A 12, 1800 (1994); J.G. Amar, F. Family, and P.-M. Lam, Phys. Rev. B 50, 8781 (1994). For a review, see ref [16] and [14].
[12] P. Jensen, A.-L. Barabasi, H. Larralde, S. Havlin, and H.E. Stanley, Nature 368, 22 (1994); Physica A 207, 219-227 (1994); Phys. Rev. B 50, 15316 (1994)
[13] G.S. Bales and D.C. Chrzan, Phys. Rev. B 50, 6057 (1994)
[14] J. Villain and A. Pimpinelli Physique de la Croissance Cristalline (Eyrolles, 1995) (english edition to be published by Cambridge University Press, 1997)
[15] P. Jensen, La Recherche 283 42 (1996)
[16] A.-L. Barabasi and H.E. Stanley, Fractal Concepts in Surface Growth (Cambridge University Press, 1995).
[17] C. Ratsch, A. Zangwill, P. Smilauer and D. Vvedensky, Phys. Rev. Lett. 72, 3194 (1994)
[18] P. Jensen, H. Larralde and A. Pimpinelli, Phys. Rev. B 55, 2556 (1997) : note that in this paper, a mistake was made in the normalization of the island size distributions (Fig. 9). This error is corrected in [38]
[19] V.N.E. Robinson and J.L. Robins, Thin Solid Films, 12, 255 (1972);
[20] M.J. Stowell, Phil. Mag. 26, 361 (1972)
[21] J.A. Venables, Phil. Mag. 27, 697 (1973)
[22] J.A. Venables, G.D.T. Spiller, and M. Hanbucken, Rep. Prog. Phys. 47, 399 (1984).
[23] S. Stoyanov and D. Kaschiev, Current Topics in Mat. Science, Ed. E. Kaldis, (North-Holland, 1981)
[24] P. Jensen, A.-L. Barabasi, H. Larralde, S. Havlin, and H.E. Stanley, Fractals (to be published, 1996)
[25] P. Jensen, L. Bardotti, A.-L. Barabasi, H. Larralde, S. Havlin, and H.E. Stanley, MRS Proceedings 407 (Fall 1995 Meeting).
[26] R. Kern, G. Le Lay and J.J. Metois, Current Topics in Mat. Science, Ed. E. Kaldis, 3 (North-Holland, 1979)
[27]
[28] C.T. Campbell, Surf. Sci. Rep. 27 1 (1997)
[29] P. Jensen and B. Niemeyer, Surf. Sci. Lett. 384 823 (1997)
[30] J.L. Robins and T.N. Rhodin, Surf. Science, 2, 346 (1964)
[31] M. Harsdor, Thin Sol. Films 116, 55 (1984)
[32] G.L. Kellogg, Phys. Rev. Lett. 73, 1833 (1994) and references therein.
[33] T.J. Raeker and A.E. DePristo, Surf. Sci. 317, 283 (1994)
[34] S. Liu, L. Bonig and H. Metiu, Phys. Rev. B 52 2907 (1995)
[35] M.C. Bartelt, S. Gunther, E. Kopatzi, R.J. Behm and J.W. Evans (to be published, Phys Rev B, 1996)
[36] W.K. Burton, N. Cabrera and F. Frank, Phil. Trans. Roy. Soc. 243, 299 (1951)
[37] G. Zinsmeister, Vacuum 16, 529 (1966); Thin Solid Films 2, 497 (1968); Thin Solid Films 4, 363 (1969); Thin Solid Films 7, 51 (1971)
[38] P. Jensen, to appear in Rev. Mod. Phys. (1998)
[39] L. Bardotti, P. Jensen, M. Treilleux, B. Cabaud and A. Hoareau, Phys. Rev. Lett. 74, 4694 (1995) ;
[40] J.A. Stroscio and D.T. Pierce, J. Vac. Sci. Technol. B 12 1783 (1994)
[41] C. Ratsch, P. Smilauer, A. Zangwill, D.D. Vvendensky, Surf. Sci. 329, L599 (1995)
[42] C.R. Henry and M. Meunier, Vacuum (to be published)

FIG. 1. Typical island morphology generated by our model.

FIG. 2. Universal function rescaling all our data. As predicted by Equation 2.28, the normalized island density $N_{max} X_S^2$ follows a single curve as a function of the evaporation parameter $(F/D)^{2/3} X_S^{10/3} (1 + X_S^2)^{2/3}$. The solid curve shows the function predicted in the text (Equation 2.28), while the circles represent the results of the computer simulations.

FIG. 3. Evolution of the maximum island density as a function of the flux for different evaporation times. The solid lines show the expected value for the exponent when evaporation is significant (2/3) while the dashed line shows the exponent in the complete condensation case (2/7).

FIG. 4. Maximum island density as a function of the evaporation time for different fluxes. The number next to each symbol corresponds to the log(F) value for that set. The solid line shows the expected value for the exponent : 2/3 for low values of $_e$ (evaporation is significant).

FIG. 5. Exponent of the mean island radius as a function of deposition time in three deposition conditions : (a) complete condensation, (b) strong evaporation (c) intermediate case. (a) shows the time exponent for the radius (filled triangles) and for the islands (open squares). We note that the exponent of the island evolution starts at 0.33 as predicted but then slightly decreases to 0.26 (b) shows the averaged time exponent of the radius (open squares) as well as the real mean values of the radius for 8 runs (to show the fluctuations). The dashed line indicates the predicted value for the exponent (1). (c) shows the values of the radius exponent for two different values of the parameters, in the intermediate regime (high evaporation at the beginning of the growth, decreasing as islands form, see below). There seems to be a typical value for the exponent of about 0.6. In all these figures, the value of the local exponent is obtained by a simple derivative in the log-log plot. The precise parameters used for each graph are : (a) $F = 10^{-11}$; $_e = 10^{15}$; $= 1/L = 1500$, averaged over 5 runs; (b) $F = 10^{-8}$; $_e = 1$; $= 1/L = 1300$, averaged over 8 runs; (c) squares : $F = 10^{-10}$; $_e = 100$; $= 1/L = 1550$, averaged over 3 runs, filled circles : $F = 10^{-8}$; $_e = 100$; $= 1/L = 1350$, averaged over 8 runs

FIG. 6. Evolution of the island density as a function of the thickness (e Ft) for different growth hypothesis. This figure shows that the same saturation density can be obtained for films grown in very different conditions. Note that the horizontal scale is logarithmic : therefore, nucleation on defects leads to saturation at extremely low coverages, almost impossible to observe experimentally. The different sets of data represent : triangles : growth with evaporation, $_e = 100$ and $F = 1.2\ 10^{-8}$, circles : growth without evaporation ($F = 3\ 10^{-10}$), and squares : growth on defects (defect concentration : $5\ 10^{-4}$ per site) and $F = 10^{-14}$ (no evaporation).

FIG. 7. Normalized island size distributions obtained for $F = 10^{-8}$ and different values of the evaporation time $_e$. The size distributions are averaged for different coverages between .05 and 0.2. The solid line shows the size distribution obtained without evaporation. The number next to each symbol corresponds to $_e =$.

FIG. 8. Effect of the presence of defects on the island size distribution. The rescaled island size distributions are obtained for $F = 10^{-8}$ and different values of the evaporation time $_e$ ($= 1$). The size distributions were obtained for different coverages between .05 and 0.15. Contrary to what is observed for homogeneous nucleation, the histograms do depend on the coverage for nucleation on defects. The solid line shows the size distribution obtained without evaporation.

FIG. 9. Values of (a) the sticking coefficient S_{sat} and (b) the thickness e_{sat} at the saturation of island density in the total coalescence limit. In the limit of low island densities, S_{sat} is a constant. However, there are crossover regimes which depend on the precise $_e$ and which are shown here. Then, from a measure of S_{sat} and N_{sat} one can get an estimate for $_e$ for the not too low island densities which correspond to many experimental cases. In the same spirit, (b) shows the evolution of e_{sat} as a function of N_{sat} in the crossover regime. The numbers correspond to the different $_e =$ used for the simulations and the solid line represents the limiting regime (see [38] for more details).

Active

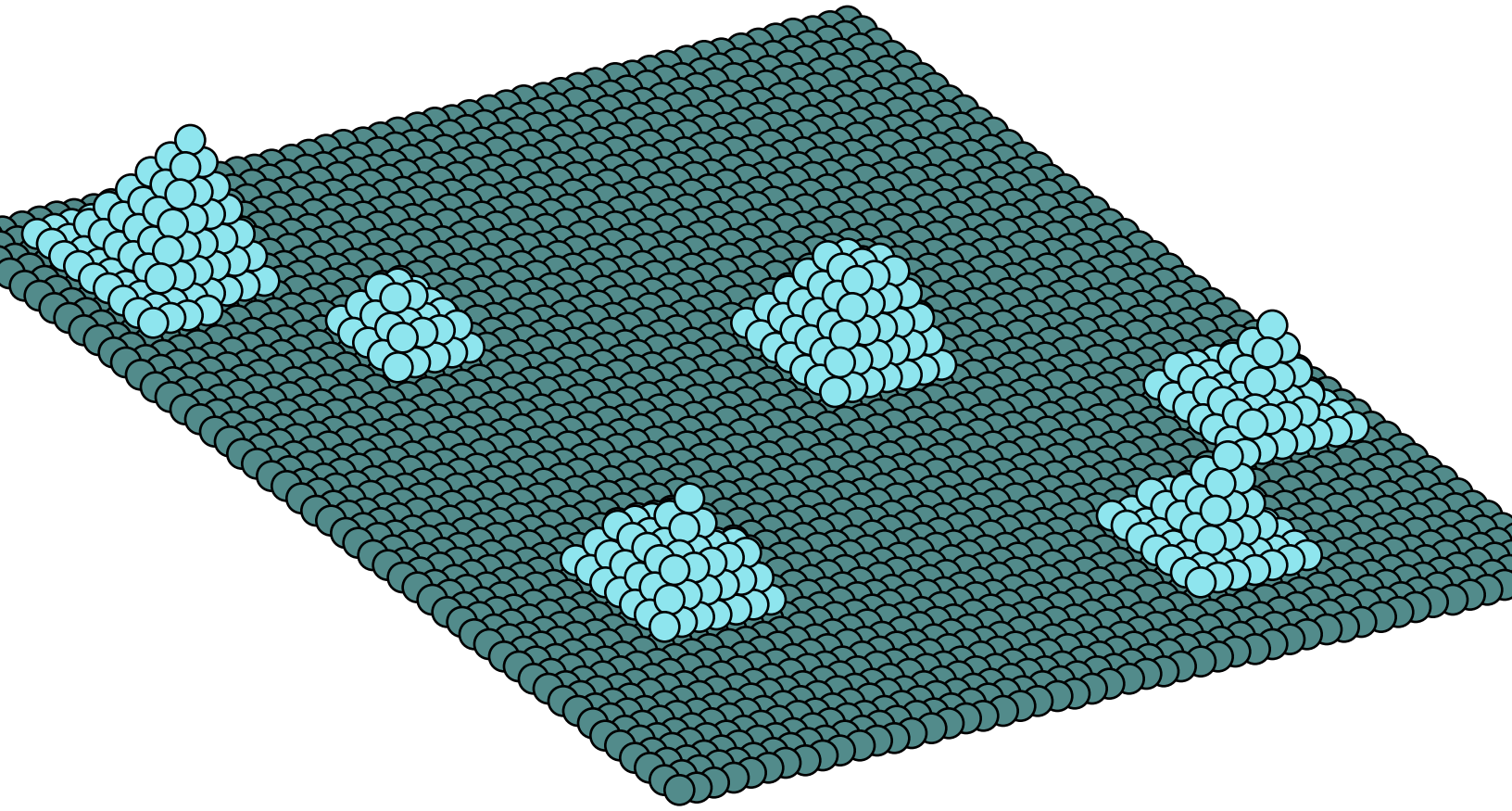

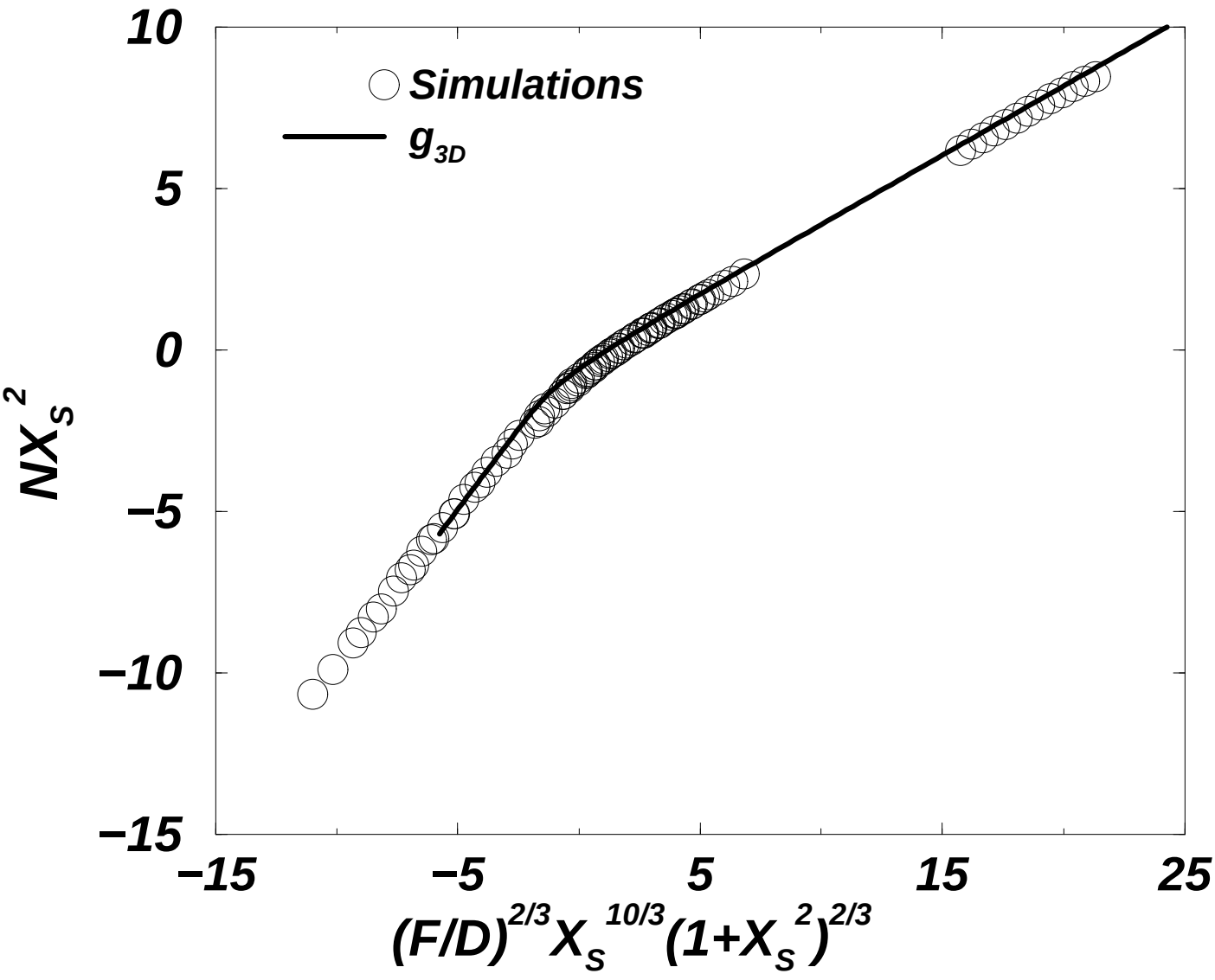
Simulations
g_{3D}
10
5
0
−5
−10
−15
−15
−5
5
15
25
NX_S^2
$(F/D)^{2/3} X_S^{10/3} (1+X_S^2)^{2/3}$

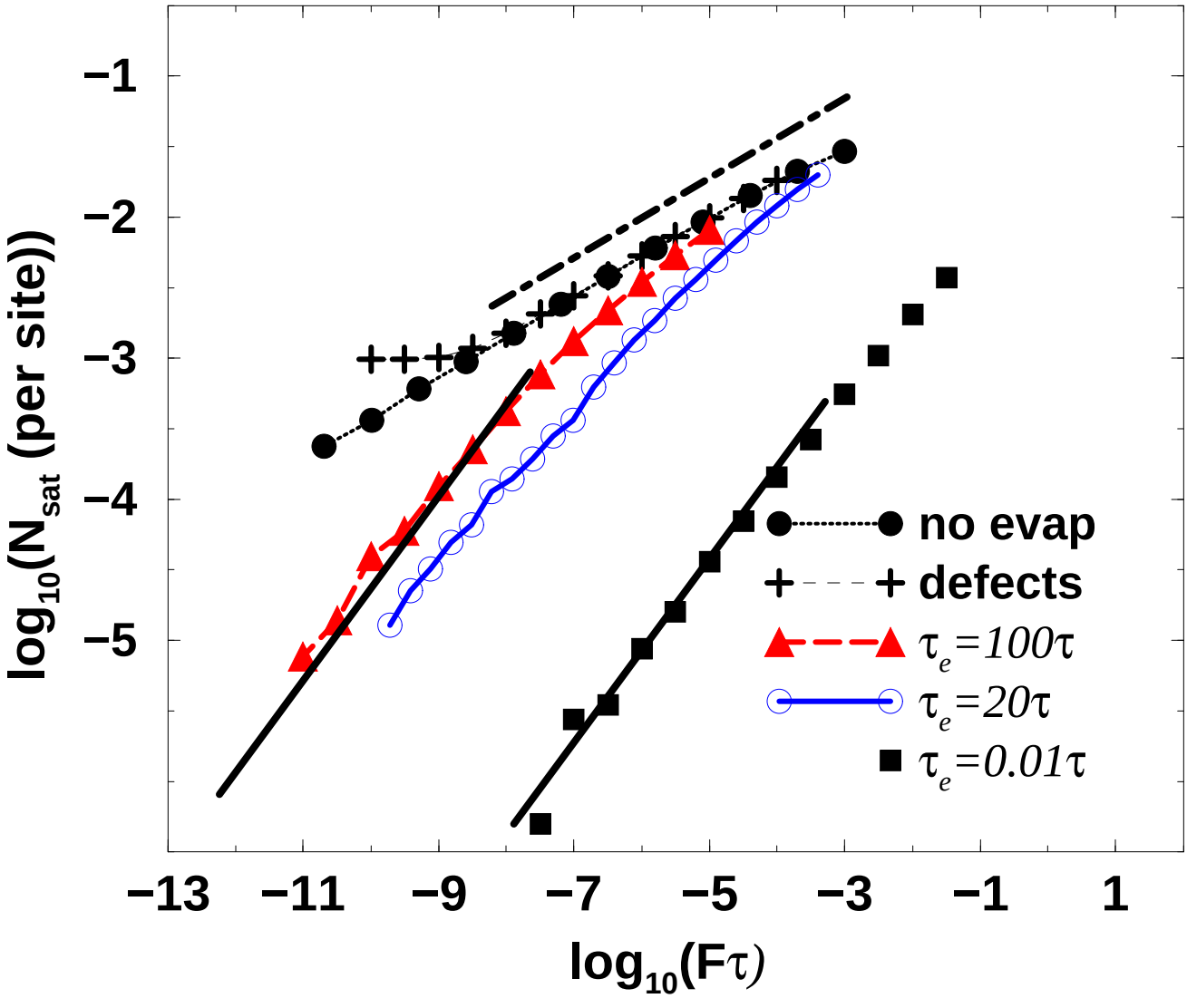
−1
−2
−3
−4
−5
log10(Nsat (per site))
−13
−11
−9
−7
−5
−3
−1
1
log10(Fτ)
no evap
defects
τe=100τ
τe=20τ
τe=0.01τ

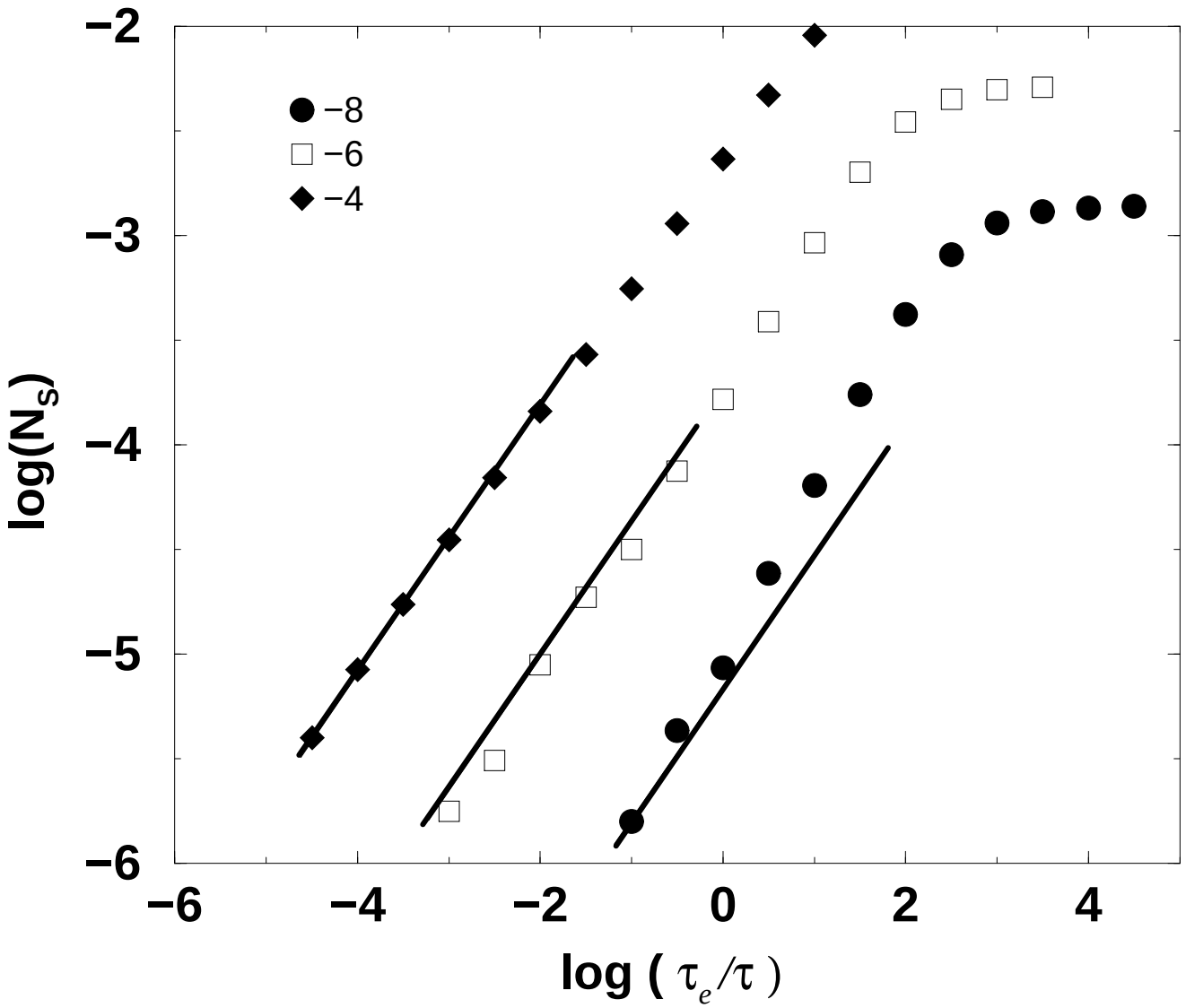

p

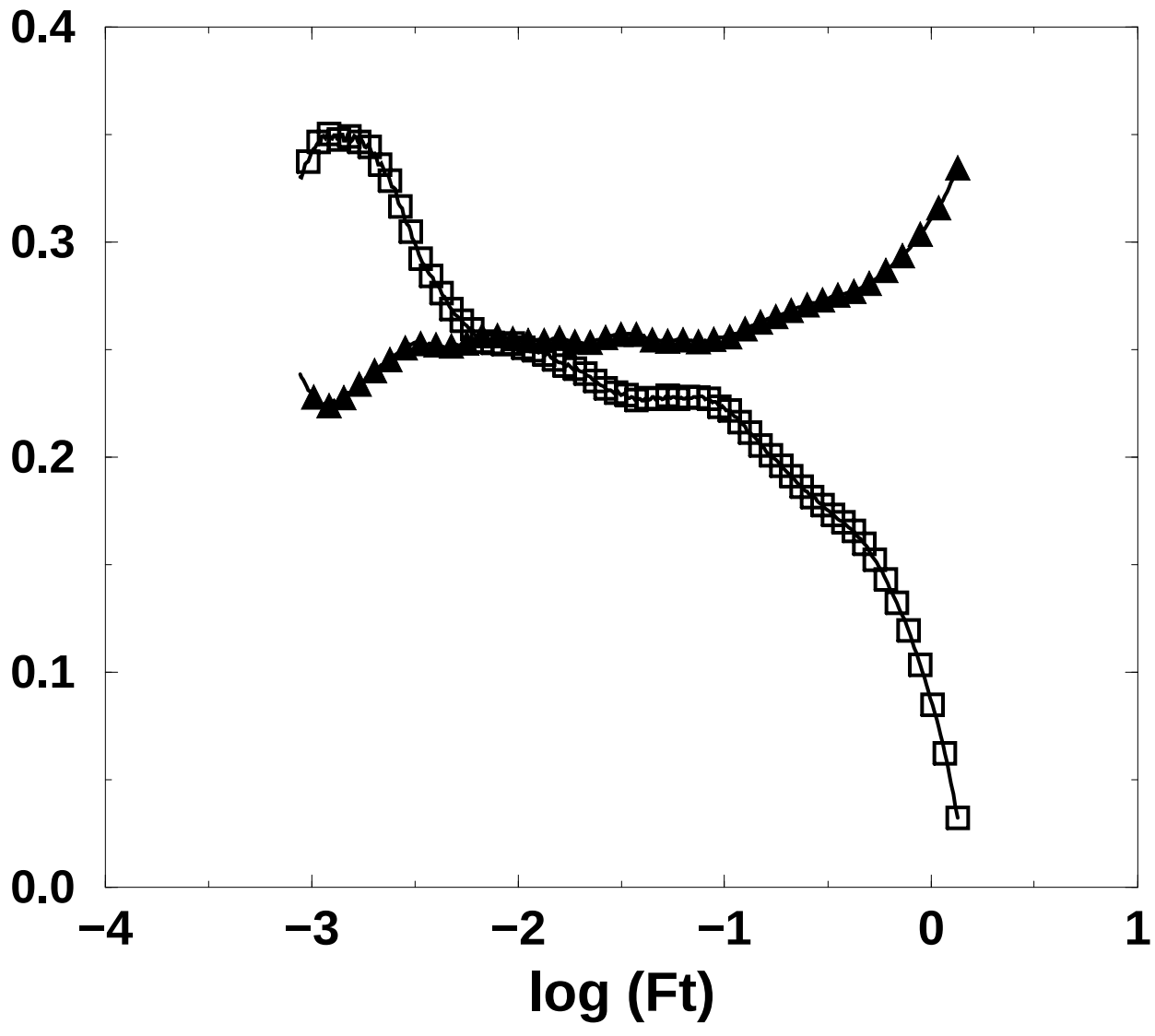
0.4
0.3
0.2
0.1
0.0
−4
−3
−2
−1
0
1
log (Ft)

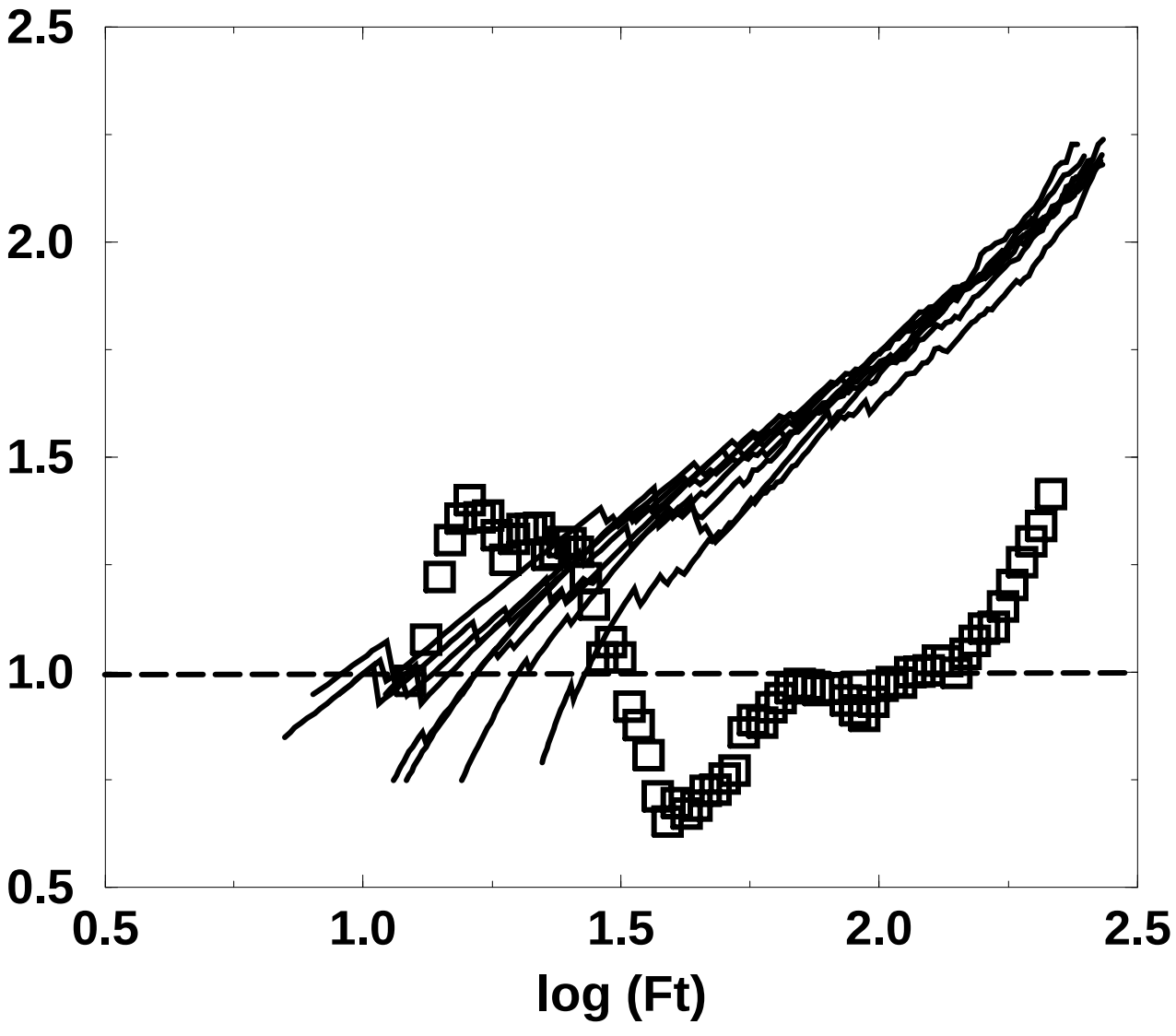
2.5
2.0
1.5
1.0
0.5
0.5
1.0
1.5
2.0
2.5
log (Ft)

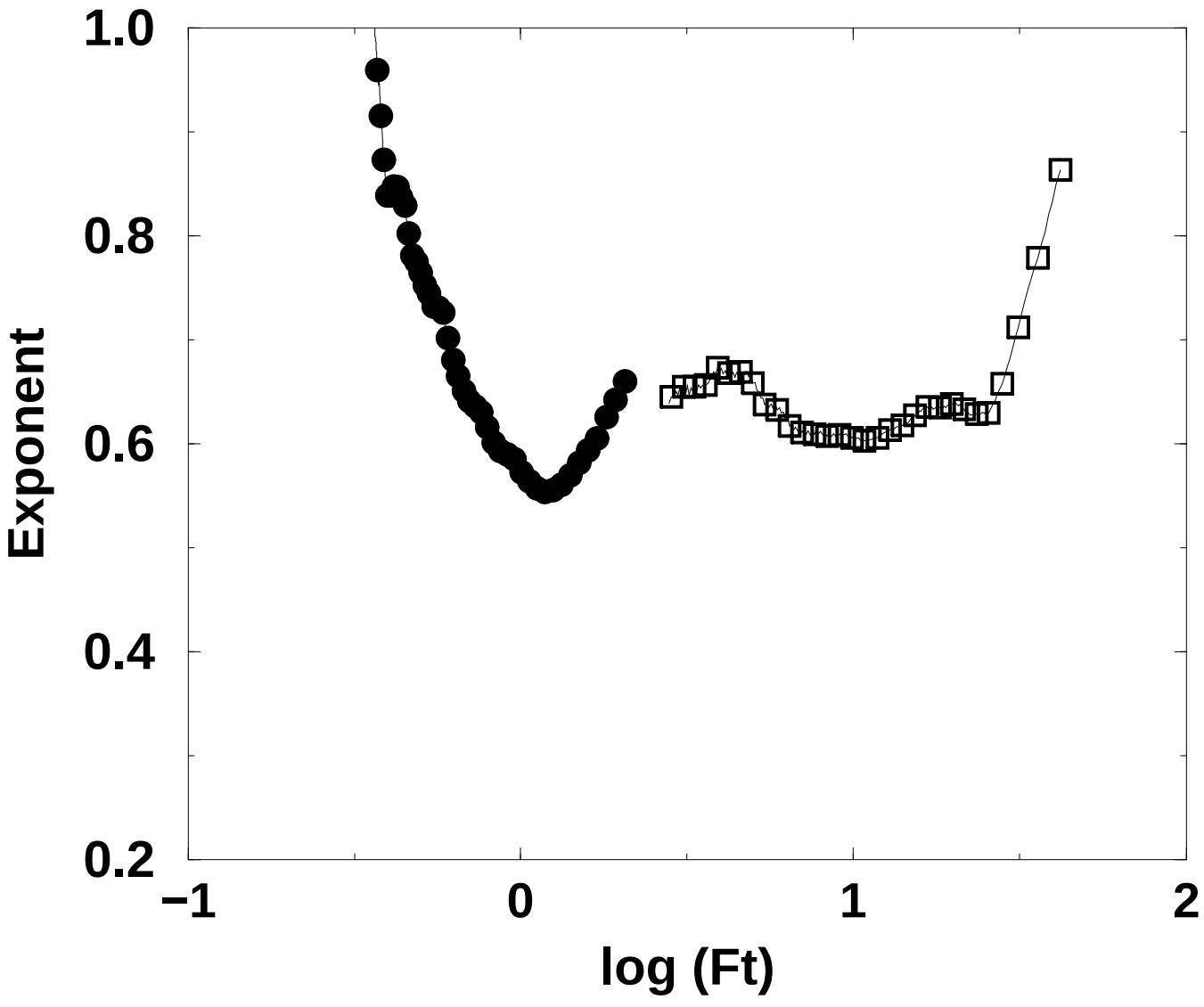
1.0
0.8
0.6
0.4
0.2
Exponent
−1
0
1
2
log (Ft)

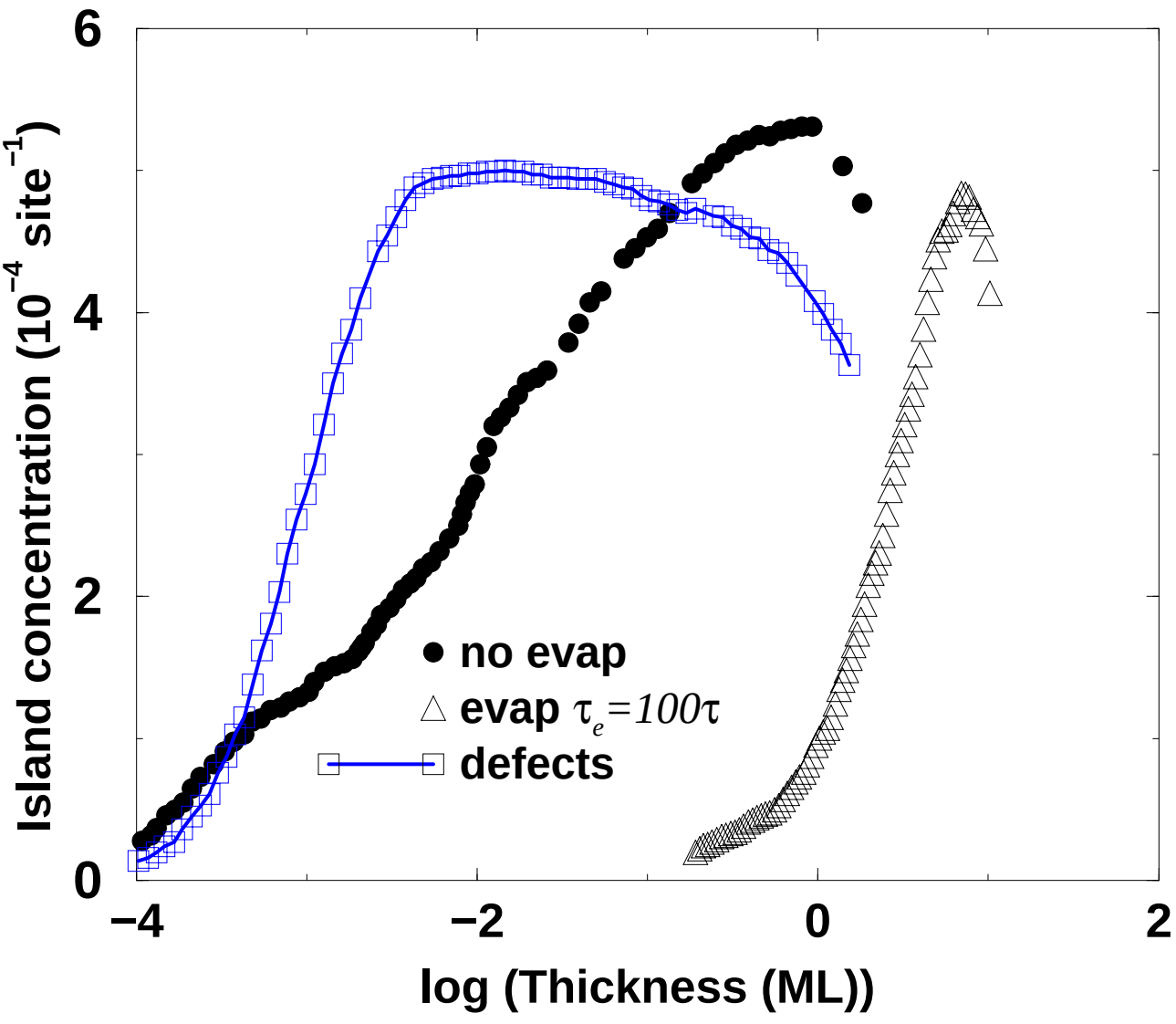
6
4
2
0
−4
−2
0
2
Island concentration (10^{-4} site^{-1})
log (Thickness (ML))
no evap
evap $\tau_e = 100\tau$
defects

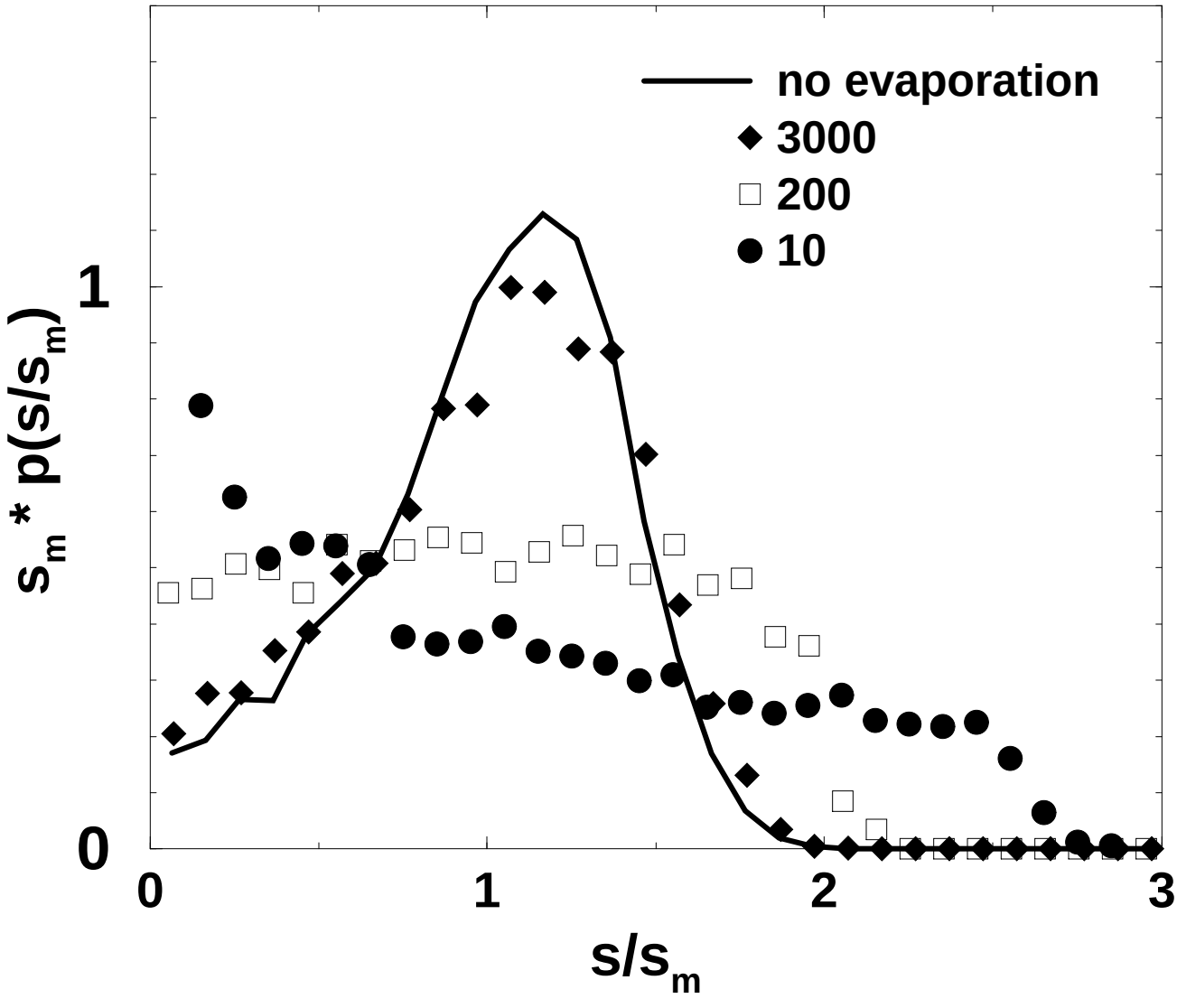
no evaporation
3000
200
10
$s_m * p(s/s_m)$
1
0
0
1
2
3
s/s_m

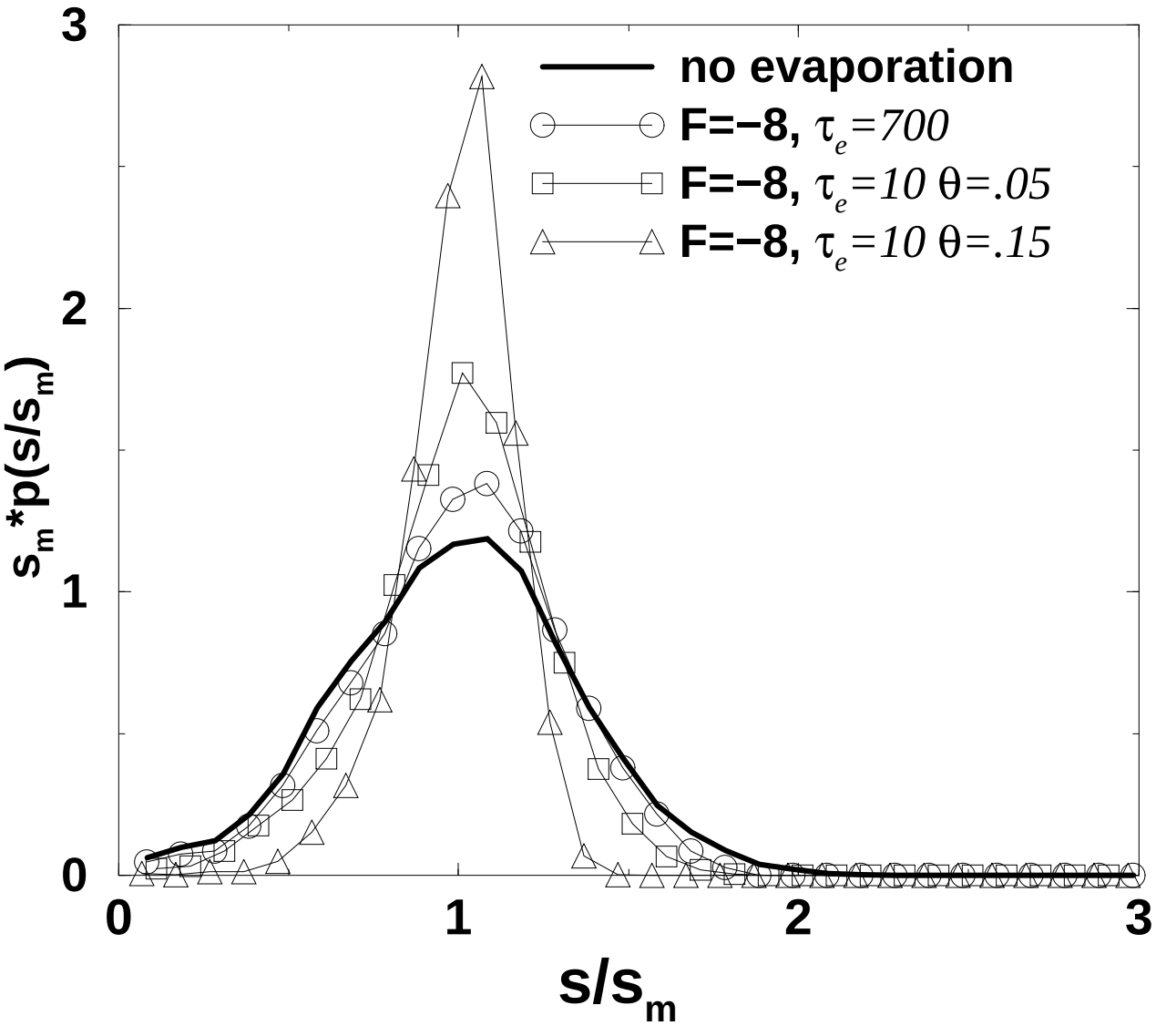
no evaporation
F=−8, τe=700
F=−8, τe=10 θ=.05
F=−8, τe=10 θ=.15
sm*p(s/sm)
s/sm
0
1
2
3
0
1
2
3

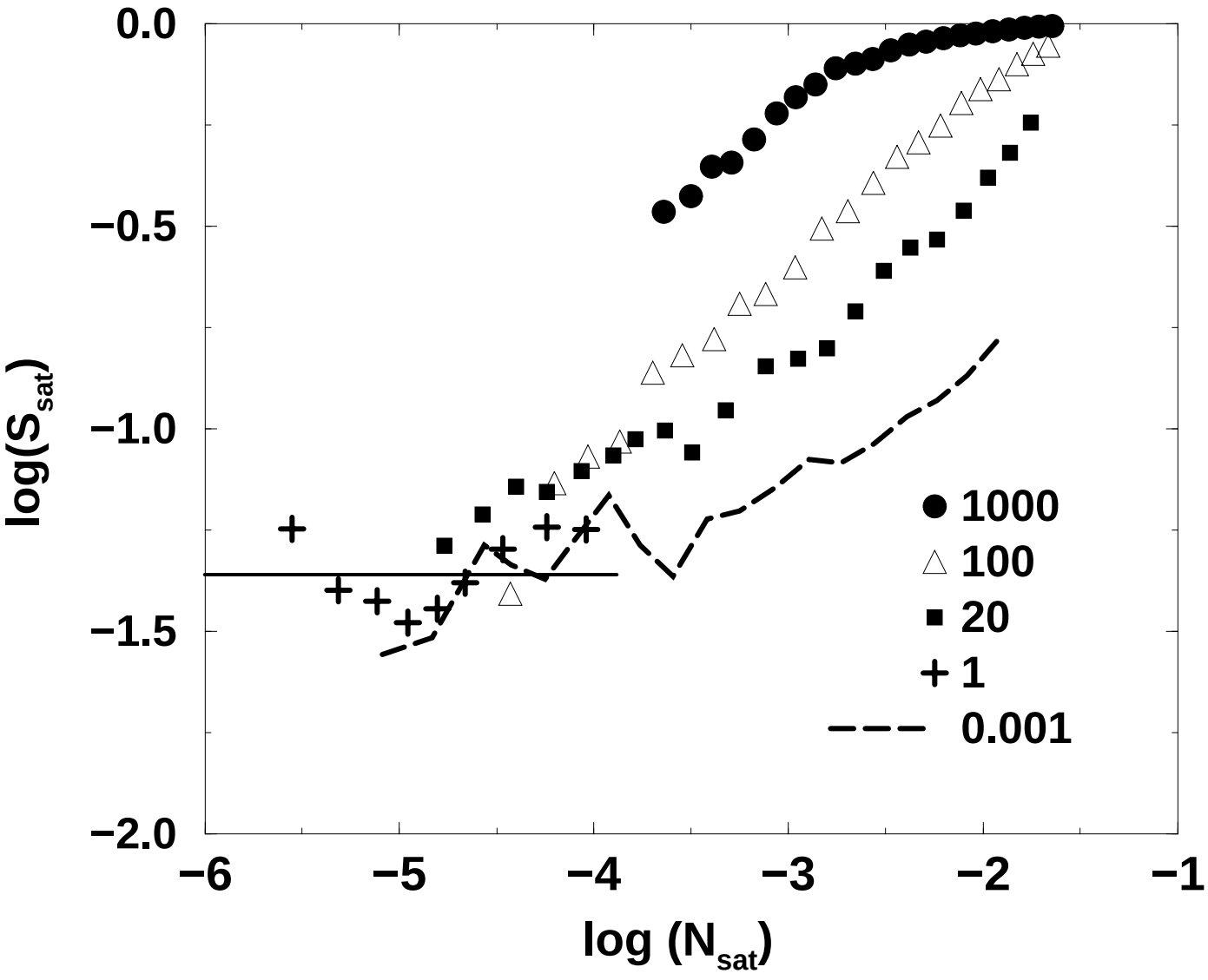
0.0
−0.5
−1.0
−1.5
−2.0
−6
−5
−4
−3
−2
−1
log(S_sat)
log (N_sat)
1000
100
20
1
0.001

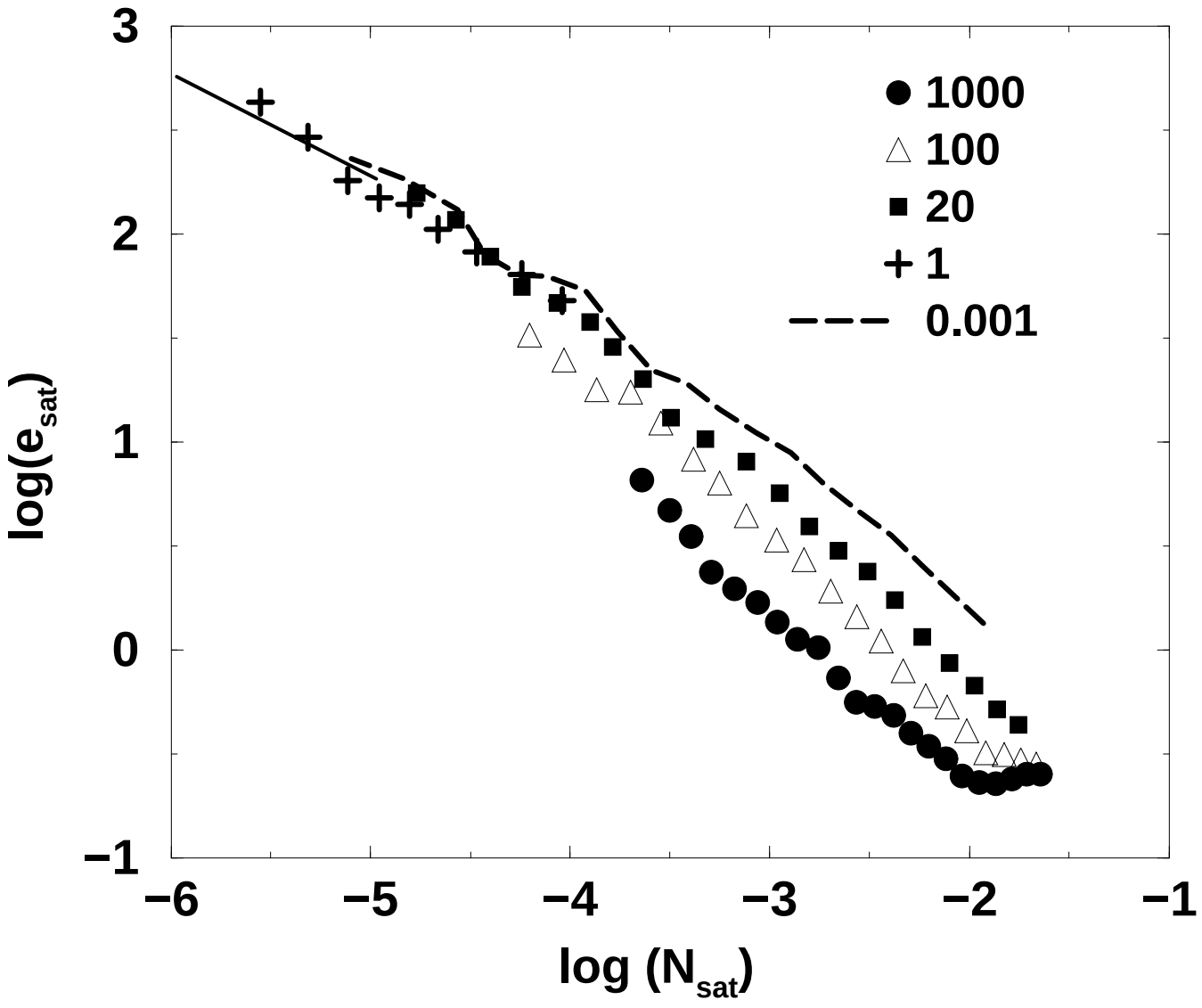
3
2
1
0
−1
−6
−5
−4
−3
−2
−1
log(e_sat)
log (N_sat)
1000
100
20
1
0.001